CANCER

Increased neutrophil extracellular trap formation promotes thrombosis in myeloproliferative neoplasms

Ofir Wolach,[1,2,3]* Rob S. Sellar,[1,4,5]* Kimberly Martinod,[6] Deya Cherpokova,[6] Marie McConkey,[1] Ryan J. Chappell,[1] Alexander J. Silver,[1] Dylan Adams,[1] Cecilia A. Castellano,[1] Rebekka K. Schneider,[1,7] Robert F. Padera,[8] Daniel J. DeAngelo,[9] Martha Wadleigh,[9] David P. Steensma,[9] Ilene Galinsky,[9] Richard M. Stone,[9] Giulio Genovese,[5,10] Steven A. McCarroll,[5,10] Bozenna Iliadou,[11] Christina Hultman,[11] Donna Neuberg,[9] Ann Mullally,[1,5,9] Denisa D. Wagner,[6] Benjamin L. Ebert[1,5,9]†

Thrombosis is a major cause of morbidity and mortality in Philadelphia chromosome–negative myeloproliferative neoplasms (MPNs), clonal disorders of hematopoiesis characterized by activated Janus kinase (JAK)–signal transducer and activator of transcription (STAT) signaling. Neutrophil extracellular trap (NET) formation, a component of innate immunity, has been linked to thrombosis. We demonstrate that neutrophils from patients with MPNs are primed for NET formation, an effect blunted by pharmacological inhibition of JAK signaling. Mice with conditional knock-in of $Jak2^{V617F}$, the most common molecular driver of MPN, have an increased propensity for NET formation and thrombosis. Inhibition of JAK-STAT signaling with the clinically available JAK2 inhibitor ruxolitinib abrogated NET formation and reduced thrombosis in a deep vein stenosis murine model. We further show that expression of PAD4, a protein required for NET formation, is increased in $JAK2^{V617F}$-expressing neutrophils and that PAD4 is required for $Jak2^{V617F}$-driven NET formation and thrombosis in vivo. Finally, in a population study of more than 10,000 individuals without a known myeloid disorder, $JAK2^{V617F}$-positive clonal hematopoiesis was associated with an increased incidence of thrombosis. In aggregate, our results link $JAK2^{V617F}$ expression to NET formation and thrombosis and suggest that JAK2 inhibition may reduce thrombosis in MPNs through cell-intrinsic effects on neutrophil function.

INTRODUCTION

The Philadelphia chromosome–negative myeloproliferative neoplasms (MPNs) encompass a group of chronic, clonal stem cell disorders with distinct disease phenotypes characterized by increased numbers of terminally differentiated blood cells. Most MPNs have a $JAK2^{V617F}$ somatic mutation, and most of the remaining cases have mutations in *MPL* or *CALR* that also activate the Janus kinase (JAK)–signal transducer and activator of transcription (STAT) signaling pathway (*1*). Thromboembolic complications are a major cause of morbidity and mortality, but the mechanistic basis for thrombophilia in these patients is not completely understood, with several pathological processes implicated (*2, 3*). An increased white blood cell count has been associated with an increased risk of thrombosis in MPN (*4–9*), and neutrophils from patients with MPNs display a number of features of enhanced activation (*3, 10–13*).

On stimulation, normal neutrophils can expel extracellular strands of decondensed DNA in complex with histones and other neutrophil granular proteins to produce neutrophil extracellular traps (NETs) (*14*). These structures have the ability to ensnare microorganisms and have also been implicated in the pathogenesis of autoimmunity and thrombosis (*15, 16*). We examined whether NET formation may be implicated in the enhanced thrombotic tendency seen in MPNs.

RESULTS

Neutrophils derived from patients with MPNs are associated with an increase in NET formation that is blunted by ruxolitinib

We observed an increase in NET formation in neutrophils from patients with MPNs compared to those from patients with myelodysplastic syndrome (MDS) as well as age-matched controls in an unbiased screen assessing various neutrophil functions including chemotaxis, phagocytosis, and oxidative burst (fig. S1, A and B). To further investigate this finding, we quantified NET formation in a larger cohort of MPN patients and controls. We stimulated isolated neutrophils with ionomycin, a calcium ionophore. NET formation was assessed quantitatively in neutrophils by identifying typical morphological changes and citrullinated histone H3 ($H3^{cit}$) expression, which is an established and widely used marker of NET formation, as described previously (*17*). Stimulated neutrophils from patients with MPNs, including those with $JAK2^{V617F}$, had a significant increase in NET formation ($P = 0.0006$; Fig. 1, A and B, fig. S1C, and tables S1 to S3). Patients receiving a JAK1/2 inhibitor had reduced NET formation, similar to that of healthy controls (Fig. 1A). Similarly, NET formation was decreased in normal neutrophils incubated in vitro with ruxolitinib (Fig. 1, C and D). Annexin V assay showed that there was no increase in early apoptosis in human neutrophils exposed to ruxolitinib, suggesting that this decrease in NETosis was not due to an increase in an alternative mechanism of cell death (fig. S1D). Because of limited patient numbers

[1]Division of Hematology, Brigham and Women's Hospital, Boston, MA 02115, USA. [2]Institute of Hematology, Davidoff Cancer Center, Beilinson Hospital, Rabin Medical Center, Petah-Tikva, Israel. [3]Sackler Faculty of Medicine, Tel-Aviv University, Tel-Aviv 49100, Israel. [4]Department of Haematology, UCL Cancer Institute, University College London, London WC1E 6DD, UK. [5]Broad Institute of the Massachusetts Institute of Technology and Harvard, Cambridge, MA 02142, USA. [6]Program in Cellular and Molecular Medicine and Division of Hematology/Oncology, Boston Children's Hospital and Department of Pediatrics, Harvard Medical School, Boston, MA 02115, USA. [7]Department of Hematology, Cancer Institute, Erasmus Medical Center, Rotterdam 2040, Netherlands. [8]Department of Pathology, Brigham and Women's Hospital, Boston Children's Hospital, and Harvard Medical School, Boston, MA 02115, USA. [9]Department of Medical Oncology, Dana-Farber Cancer Institute, Boston, MA 02115, USA. [10]Department of Genetics, Harvard Medical School, Boston, MA 02115, USA. [11]Department of Medical Epidemiology and Biostatistics, Karolinska Institute, Stockholm SE-171 76, Sweden.
*These authors contributed equally to this work.
†Corresponding author. Email: bebert@partners.org

Fig. 1. Neutrophils derived from patients with MPNs are associated with an increase in NET formation and a prothrombotic, NET-rich phenotype. (**A**) NET formation in patients with myeloproliferative neoplasms (MPNs) (receiving a JAK inhibitor, $n = 5$; receiving other therapy, $n = 14$) compared to healthy controls ($n = 11$) when stimulated with 4 μM ionomycin (IO) or dimethyl sulfoxide (DMSO) for 2 hours. Patients receiving a JAK inhibitor are indicated by JAKI. Data are shown as individual values and medians. (**B**) Representative IF images of human neutrophils after stimulation with 4 μM IO or DMSO for 2 hours. 4′,6-Diamidino-2-phenylindole (DAPI) is shown in blue, and citrullinated histone H3 (H3^{cit}) is shown in green. Scale bar, 50 μm. (**C**) Percentages of human neutrophils with evidence of NET formation after stimulation with phorbol 12-myristate 13-acetate (PMA) (10 nM) with and without ruxolitinib pretreatment ($n = 4$). Neutrophils are derived from controls. (**D**) Representative images of human neutrophils from healthy controls stimulated with PMA (10 nM) after 150 min of ex vivo pretreatment with DMSO, ruxolitinib (300 nM), or GSK484 (PAD4 inhibitor, 10 μM). Scale bar, 50 μm. (**E**) Lung tissue sections from mice expressing the $Jak2^{V617F}$ mutation as compared to $Jak2^{WT}$ mice. Scale bar, 200 μm. (**F**) Characterization of clot content in the lungs of $Jak2^{V617}$ mice. Hematoxylin and eosin (H&E) stain. Scale bar, 50 μm. VWF, von Willebrand factor. (**G**) Lung tissue sections from mice expressing the $Jak2^{V617F}$ mutation as compared to $Jak2^{WT}$ mice. Neutrophil infiltration and NETs are shown by neutrophil-specific Ly6G (red) and H3^{cit} (green), respectively. Scale bar, 100 μm. (**H**) Percentages of mouse neutrophils with evidence of NET formation by morphological criteria (left) ($n = 9$ for all genotype/treatment combinations) or H3^{cit}-positive staining (right) ($n = 6$ for all genotype/treatment combinations) grouped by genotype after stimulation with 4 μM IO or DMSO for 2 hours. (**I**) Representative IF images of mouse neutrophils derived from $Jak2^{WT}$ and $Jak2^{V617F}$ mice after stimulation with 4 μM IO or DMSO for 2 hours. DAPI is shown in blue, and H3^{cit} is shown in green. Scale bar, 50 μm.
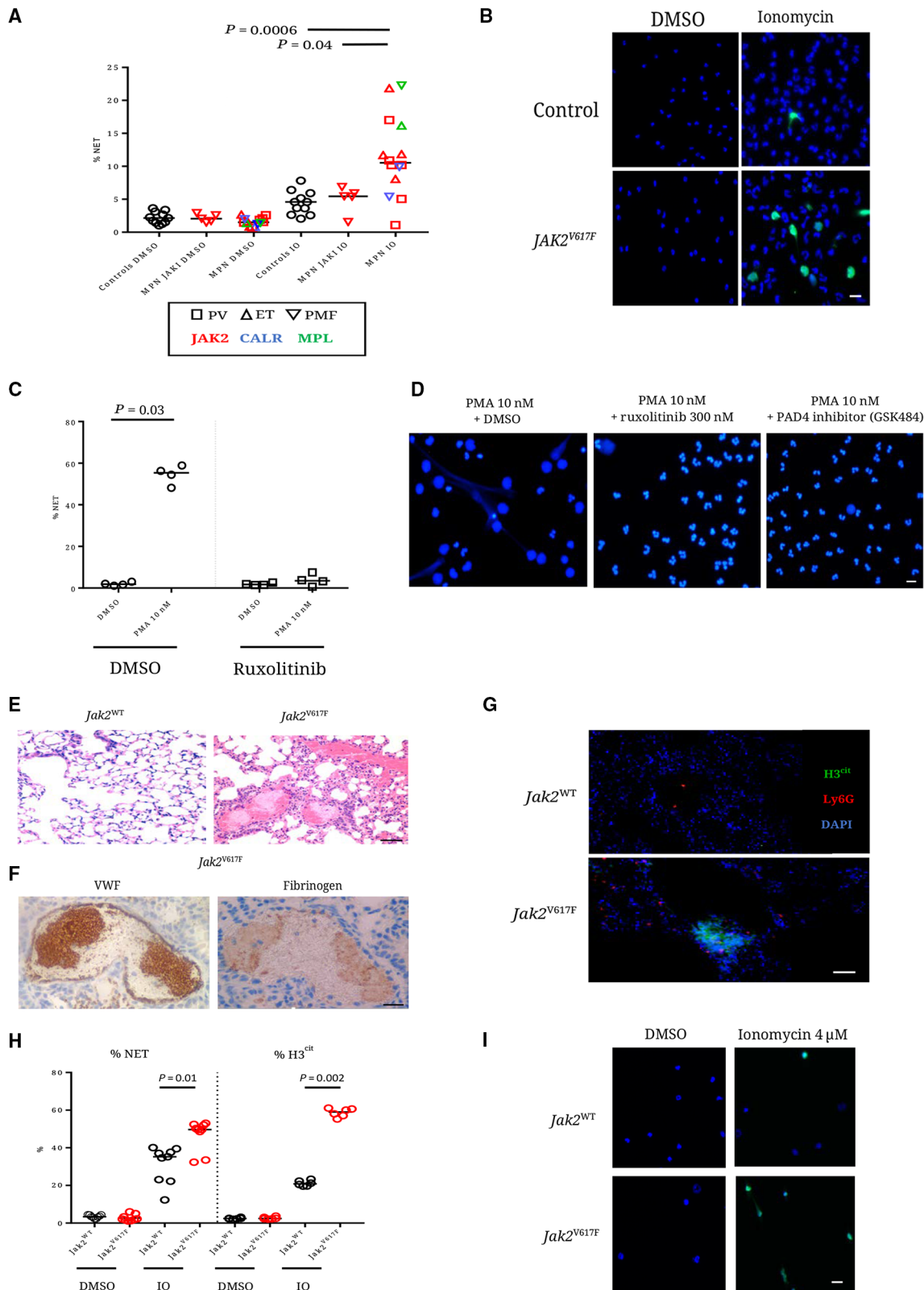
receiving hydroxyurea, and no patients receiving interferon, the effects of these therapies on NET formation could not be assessed.

$Jak2^{V617F}$-driven MPN mouse models have a NET-rich, prothrombotic phenotype

To validate our findings from primary MPN samples in a genetically controlled, in vivo experimental model, we used an established conditional knock-in murine model for the $Jak2^{V617F}$ allele (18). $Jak2^{V617F/WT}$;Vav-Cre mice, with heterozygous expression of the $Jak2^{V617F}$ allele in hematopoietic cells (abbreviated as $Jak2^{V617F}$), develop an MPN phenotype reminiscent of human polycythemia vera (PV) and have a shortened life span (18). We first determined whether $Jak2^{V617F}$ mice develop spontaneous pulmonary thrombosis using immunohistochemical (IHC) assessment of lung sections. We found increased thrombosis in $Jak2^{V617F}$ mice, whereas $Jak2^{WT}$ mice had no evidence of spontaneous thrombosis in the lungs (Fig. 1, E and F).

To determine whether the pathologic thrombosis was associated with NET formation, we used immunofluorescence (IF) to assess neutrophil infiltration and expression of H3^{cit}, an established marker of NET formation. We found an increase in H3^{cit} expression in the lungs of $Jak2^{V617F}$ mice (Fig. 1G). Furthermore, neutrophils isolated from the peripheral blood of $Jak2^{V617F}$ mice had a significant increase in NET formation upon stimulation with ionomycin ($P = 0.01$; Fig. 1, H and I).

Ruxolitinib reduces the rate of induced venous thrombosis in $Jak2^{V617F}$-driven MPN mouse models

To interrogate the propensity for acute thrombosis in $Jak2^{V617F}$ mice, we assessed thrombosis after experimental stenosis of the inferior vena cava (IVC), an established model for determining predisposition to venous thrombosis that has previously been shown to be NET-dependent (19). To ensure that the observed effects were a result of cell-intrinsic properties of $Jak2^{V617F}$-expressing neutrophils, we isolated c-Kit–positive cells from $Jak2^{V617F}$ mice and transplanted them into lethally irradiated $Jak2^{WT}$ recipient mice. As expected, recipient mice developed a PV-like phenotype with high hematocrit (HCT) and enlarged spleens (fig. S2). Recipient mice were then treated for 72 hours with ruxolitinib or vehicle.

Mice engrafted with $Jak2^{V617F}$-expressing hematopoietic cells had a marked predisposition to thrombosis. At 2 hours after partial ligation of the IVC, 45% of Jak2^{V617F} vehicle-treated mice developed thrombosis, whereas none of the $Jak2^{WT}$ mice had evidence of thrombosis ($P = 0.04$; Fig. 2, A and B). Plasma concentrations of double-stranded DNA (dsDNA), a marker of NET activity, were increased in Jak2^{V617F} as compared to $Jak2^{WT}$ mice (Fig. 2C). At 4 hours, thrombosis rates were not significantly different in the $Jak2^{V617F}$ as compared to $Jak2^{WT}$ mice (71% versus 60%, respectively; $P = 0.7$). The thrombi seen in the $Jak2^{V617F}$ mice had an increase in H3^{cit} and neutrophil content as compared to $Jak2^{WT}$ mice (Fig. 2, D and E, and fig. S3, A and B). No qualitative differences were noted in the amount or pattern of platelet staining, fibrin, or red blood cell (RBC) content between $Jak2^{WT}$ and $Jak2^{V617F}$ mice (fig. S3, C and D).

Ruxolitinib decreased the rate of thrombosis in $Jak2^{V617F}$ mice after IVC stenosis. At 2 hours post-IVC ligation, after 72 hours of ruxolitinib treatment, the ruxolitinib-treated mice had significantly lower thrombosis rates compared to vehicle-treated $Jak2^{V617F}$ mice (Fig. 2A; 0% versus 45%, respectively; $P = 0.04$). At 4 hours, ruxolitinib treatment significantly reduced thrombosis in $Jak2^{V617F}$ mice (Fig. 2A; 21% versus 71%; $P = 0.02$). Furthermore, the amount of H3^{cit} as well as neutrophil content within the thrombi were significantly reduced in ruxolitinib-treated

$Jak2^{V617F}$ as compared to vehicle-treated mice ($P = 0.009$ and $P = 0.001$, respectively; Fig. 2, D and E, and fig. S3, A and B). Ruxolitinib treatment did not significantly affect the HCT, neutrophil, or platelet counts, all potential contributors to a thrombotic phenotype (Fig. 2F).

To further investigate the contribution of NETs to the thrombotic tendency in the partial ligation model, we assessed clot formation rate after treatment with vehicle or deoxyribonuclease (DNase; Pulmozyme, Genentech). DNase has been previously shown to disrupt NET structures and protect mice from thrombus formation in NET-dependent models (20, 21). $Jak2^{V617F}$ mice treated with DNase had lower thrombus formation rates than vehicle-treated mice (zero of eight clots and five of seven clots in the DNase- and vehicle-treated mice, respectively; $P = 0.007$). Thrombus formation rates were 63 and 14% for $Jak2^{WT}$ vehicle- and DNase-treated mice, respectively (five of eight clots and one of seven clots in the vehicle- and DNase-treated mice, respectively; $P = 0.06$) (fig. S4A). There was no significant decrease in the concentration of dsDNA in plasma from $Jak2^{WT}$ or $Jak2^{V617F}$ mice after DNase treatment (fig. S4B). There was no evidence of H3^{cit} in thrombi from $Jak2^{WT}$ mice after treatment with vehicle or DNase (fig. S4C). Again, there was diffuse H3^{cit} in thrombi from $Jak2^{V617F}$ mice (fig. S4C). However, because no $Jak2^{V617F}$ mice treated with DNase formed thrombi, we were unable to assess H3^{cit} in this setting.

We repeated our thrombosis experiments in a full ligation ("stasis") model that was previously shown to be associated with NET-independent thrombus formation (fig. S5) (22, 23). At 4 hours, no difference in clotting rate was noted between vehicle- and ruxolitinib-treated $Jak2^{WT}$ mice (four of six and five of six clots for vehicle- and ruxolitinib-treated, respectively; $P = 0.33$) (fig. S6A). Furthermore, no differences in the patterns of platelet and H3^{cit} staining were noted on IF studies or in the measurements of plasma dsDNA ($P = 0.48$) (fig. S6, B and C). No clots were observed in any of the $Jak2^{V617F}$ mice treated with vehicle or ruxolitinib (zero of four and zero of five, respectively) (fig. S6A).

To further evaluate aspects of neutrophil activation, we assessed the formation of reactive oxygen species (ROS) [using dihydrorhodamine (DHR)] and CD11b expression in $Jak2^{WT}$ and $Jak2^{V617F}$ mice. No differences were observed between $Jak2^{WT}$ and $Jak2^{V617F}$ mice at baseline or after ionomycin treatment, and there was no evidence of decreased baseline concentrations or post-stimulation concentrations in neutrophils from mice treated for 72 hours with ruxolitinib (fig. S7).

To assess a potential impact of genotype or treatment on platelet function in our model, we performed platelet aggregometry (fig. S8, A and B). Platelets from $Jak2^{V617F}$ were hyporeactive as compared to $Jak2^{WT}$ mice with reduced maximal aggregation responses for activation after stimulation with adenosine diphosphate (ADP), collagen, or thrombin. To assess whether this reflected $Jak2^{V617F}$ platelets that were already maximally activated, we performed assays of activation at baseline and after thrombin stimulation, as assessed by measurement of surface expression of P-selectin and αIIb/βIII. There was no evidence that platelets from $Jak2^{V617F}$ had increased baseline activation, and reduced activation after stimulation was again demonstrated (fig. S8C). These findings are in line with previous reports of hyporeactive platelets in $Jak2^{V617F}$ mice (24).

PAD4 is overexpressed in MPNs and is essential for the NET-driven prothrombotic phenotype in $Jak2^{V617F}$-driven MPN mouse models

Chromatin decondensation is an essential step for NET formation. One mechanism by which this occurs is the activation and nuclear localization of peptidyl-arginine deiminase (PAD4), resulting in the
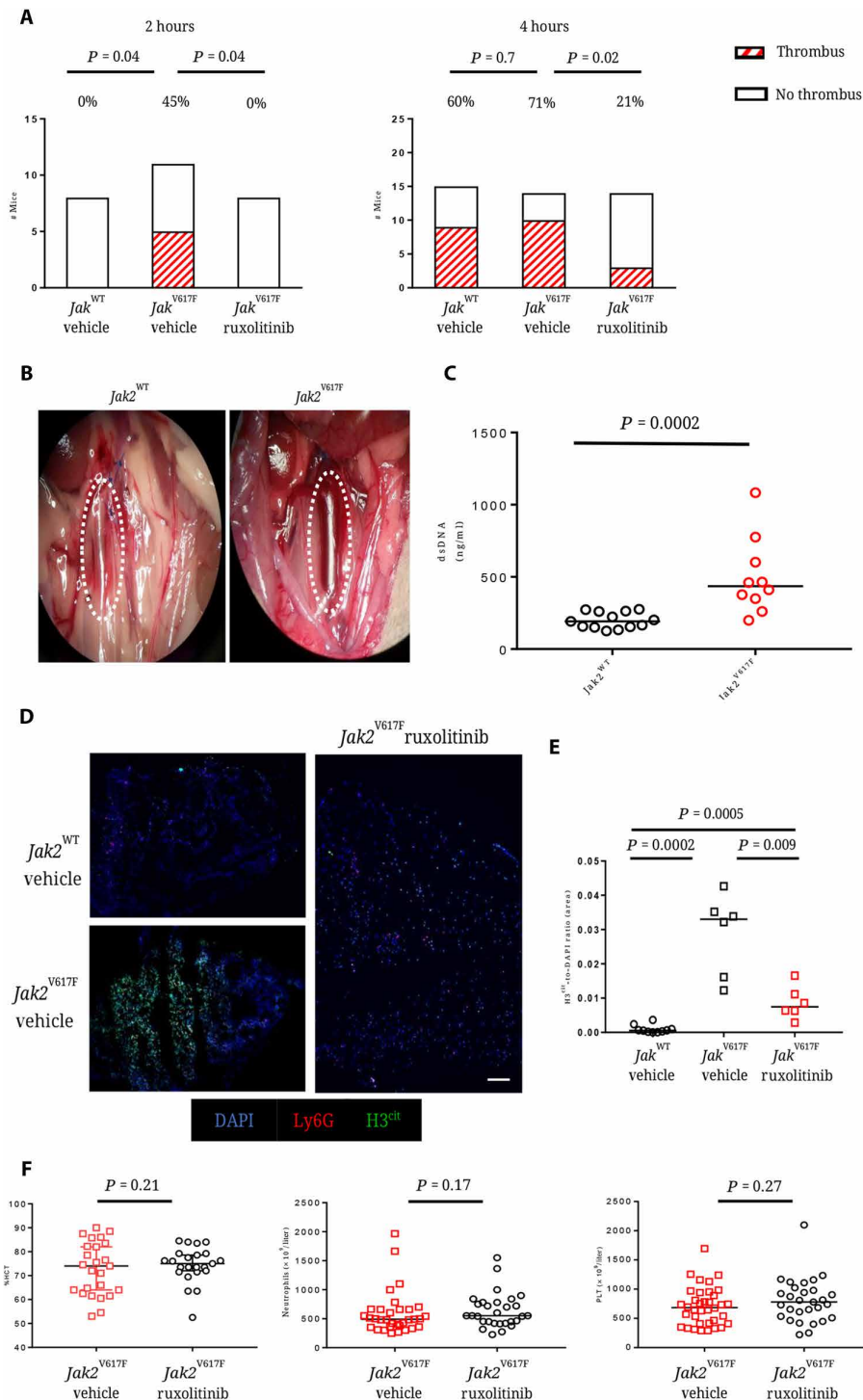
Fig. 2. *Jak2*^V617F is associated with increased venous thrombosis tendency that is reversed with ruxolitinib. (**A**) Rates of thrombosis at 2 and 4 hours after surgical stenosis of the IVC, with animals grouped according to genotype and in vivo treatment (vehicle or ruxolitinib, 90 mg/kg twice a day for 72 hours). At 2 hours: $Jak2^{WT}$ vehicle, $n = 8$; $Jak2^{V617F}$ vehicle, $n = 11$; $Jak2^{V617F}$ ruxolitinib, $n = 8$. At 4 hours: $Jak2^{WT}$ vehicle, $n = 15$; $Jak2^{V617F}$ vehicle, $n = 14$; $Jak2^{V617F}$ ruxolitinib, $n = 14$. (**B**) Representative image at 2 hours after IVC stenosis in a $Jak2^{WT}$ mouse and a $Jak2^{V617F}$ mouse. (**C**) dsDNA plasma concentration in $Jak2^{WT}$ ($n = 13$) and $Jak2^{V617F}$ ($n = 10$) mice subjected to partial stenosis of the IVC. (**D**) Neutrophil infiltration and NET content of sections of thrombi harvested at 4 hours after IVC stenosis, as shown by neutrophil-specific Ly6G (red) and H3^cit (green), respectively. DAPI is shown in blue. Scale bar, 100 μm. (**E**) Percentage of cells (DAPI) staining positively for H3^cit in thrombi harvested at 4 hours after IVC stenosis. (**F**) HCT, neutrophil count, and platelet count (PLT) in $Jak2^{V617F}$ mice after 72 hours of treatment with vehicle ($n = 36$) or ruxolitinib (90 mg/kg twice a day; $n = 29$).

citrullination of histones. Inhibition of this pathway abrogates NET formation in murine models (*25, 26*). To determine the role of PAD4 in $Jak2^{V617F}$-driven NET formation and thrombosis, we used an established $Jak2^{V617F}$ retroviral bone marrow transplant model (*27*). We transduced c-Kit–positive bone marrow cells from *Pad4* null (*Pad4^{−/−}*) mice (*26*) with $Jak2^{V617F}$ retrovirus and transplanted the cells into lethally irradiated $Jak2^{WT}$ recipients. As in other models with *Pad4* inactivation (*19*), neutrophils from mice engrafted with $Jak2^{V617F}$-expressing *Pad4* null cells did not form NETs (fig. S9). Mice with $Jak2^{V617F}$-expressing *Pad4^{+/+}* cells and mice with $Jak2^{V617F}$-expressing *Pad4^{−/−}* cells both showed similar increases in HCT as compared to $Jak2^{WT}$-expressing mice (fig. S10). Although thrombi were evident in the lungs from mice engrafted with $Jak2^{V617F}$-expressing *Pad4^{+/+}* cells, there was no evidence of thrombus in lungs from $Jak2^{V617F}$-expressing *Pad4^{−/−}* mice (Fig. 3A). In addition, there was no evidence of H3^cit in the lungs of $Jak2^{V617F}$-expressing *Pad4^{−/−}* mice (Fig. 3B). These findings demonstrate that $Jak2^{V617F}$-driven NET formation and thrombosis are dependent on PAD4. These findings also provide further evidence of a role for neutrophils in causing thrombosis in $Jak2^{V617F}$-driven MPN and are consistent with a previously reported finding that isolated polycythemia in mice (induced with exogenous erythropoietin administration) is insufficient for thrombus formation (*24*).

Because high expression of PAD4 has previously been linked to an increased propensity for NET formation (*28, 29*), we examined PAD4 expression in MPN patients. Analysis of published gene expression profiling data from neutrophils derived from MPN patients and healthy controls revealed that neutrophils from patients with homozygous $JAK2^{V617F}$ MPN had 2.4-fold higher *PAD4* RNA expression (*30*). We also found that PAD4 protein expression is increased in neutrophils from patients with $JAK2^{V617F}$ PV as compared to healthy controls (Fig. 3C).

JAK2^V617F-positive clonal hematopoiesis is associated with increased thrombosis rates

Recent studies have demonstrated that clonal somatic mutations, including $JAK2^{V617F}$, can be present in the blood of otherwise healthy individuals, a state that has been
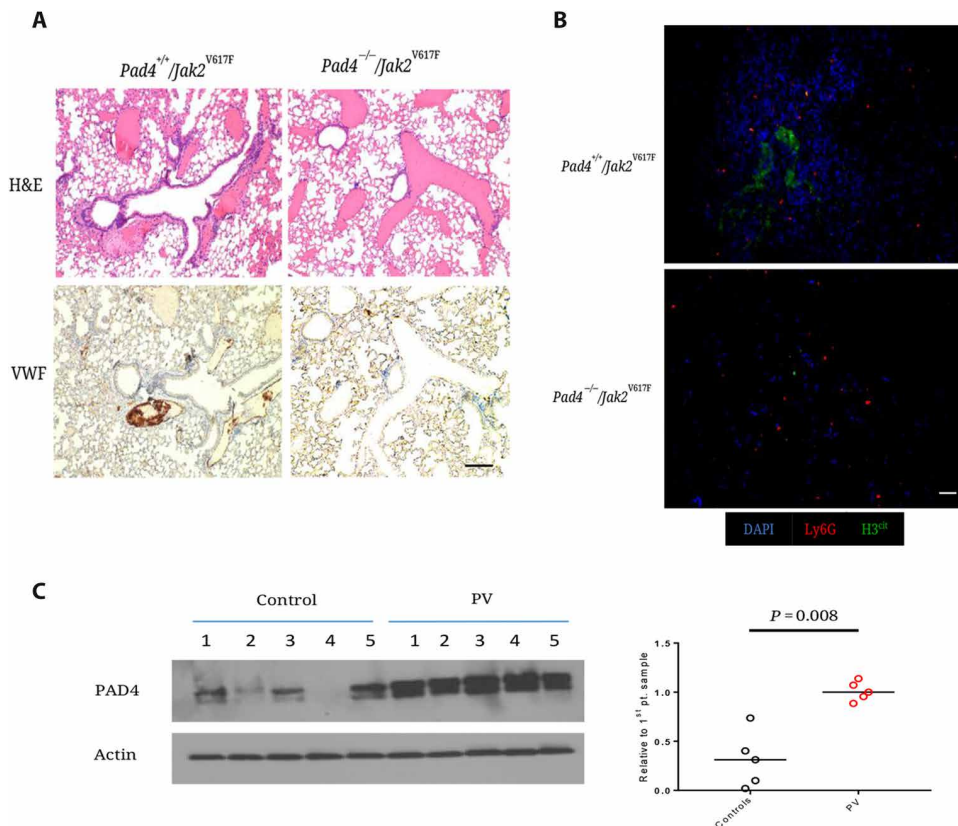
Fig. 3. PAD4 is overexpressed in MPNs and is essential for the NET-driven prothrombotic phenotype in *Jak2*^{V617F}-driven MPN mouse models. (**A**) Lung sections from mice 10 weeks after transplantation with *Pad4*$^{+/+}$ or *Pad4*$^{-/-}$ c-Kit–positive cells transduced with *Jak2*^{V617F} vector. H&E stain. Scale bar, 200 μm. (**B**) IF studies of lung sections from mice 10 weeks after transplantation with *Pad4*$^{+/+}$ or *Pad4*$^{-/-}$ c-Kit cells transduced with *Jak2*^{V617F} vector. IF studies demonstrate H3^{cit} depositions in the background of a hypercellular lung section in *Pad4*$^{+/+}$/*Jak2*^{V617F} mice as compared to *Pad4*$^{-/-}$/*Jak2*^{V617F} mice. Neutrophil infiltration and NETs are shown by neutrophil-specific Ly6G (red) and H3^{cit} (green), respectively. DAPI is shown in blue. Scale bar, 100 μm. (**C**) PAD4 protein expression and quantification in neutrophils isolated from healthy controls and patients with PV harboring the *JAK2*^{V617F} mutation (β-actin used as loading control; representative image of three technical replicates; *n* = 5 for both groups).

termed clonal hematopoiesis of indeterminate potential (CHIP) (*31*, *32*). We hypothesized that individuals with *JAK2*^{V617F}-positive CHIP, without MPN or other hematologic malignancy, may also have an increased propensity for venous thrombosis due to the presence of a population of clonal neutrophils that is primed to produce NETs.

To test this hypothesis, we examined the association between *JAK2*^{V617F}-positive CHIP and venous thrombosis in a previously described large case-control cohort that included healthy controls and patients with schizophrenia (*31*). After excluding patients with a diagnosis of a myeloid blood disorder, including MPN, 10,893 individuals had both clinical and exome sequencing data available (Fig. 4A). Excluding those with a diagnosis of MPN, *JAK2*^{V617F}-mutant CHIP was powerfully associated with major venous thrombotic events, including deep venous thrombosis and pulmonary embolus, which occurred in 25% of such cases (*n* = 4 of 16, *P* = 0.0003 as compared to non-CHIP), a rate much higher than in individuals with CHIP bearing other somatic mutations (*n* = 11 of 250, *P* = 0.02; Fig. 4B and tables S4 and S5). This association was not significant in the schizophrenic group considered in isolation (*n* = 4946), potentially because of an increased baseline incidence of thrombosis in the schizophrenia versus control cohort without CHIP (2.5% versus 1.8%; *P* = 0.02) that masks an effect (Table 1).

Thrombotic events occurred even in individuals with *JAK2*^{V617F}-positive CHIP and a low variant allele frequency (VAF) (range, 7 to 26%) (Fig. 4C). In three patients, DNA sampling postdated the initial documented thrombotic event, suggesting that thrombosis cannot be attributed to a subsequent large clonal expansion. It is noteworthy that patients with CHIP were older at the time of DNA sampling than those without CHIP (median, 65 versus 55; *P* < 0.0001); however, this age difference was seen in both those with thrombosis (65.5 versus 58.5; *P* = 0.0002) and those without (65 versus 55; *P* < 0.0001) (fig. S11). These data suggest that *JAK2*^{V617F} mutations, even at a low VAF and in the absence of demonstrable MPN or other hematologic malignancy, are associated with increased risk of major venous thrombotic events. These cases might provide a basis for some cases of spontaneous thrombosis in the general population.

DISCUSSION

NETs have previously been linked to the pathogenesis of thrombosis (*15*). Here, we offer a mechanism for the thrombotic tendency observed in MPNs. We show that *JAK2*^{V617F} expression is associated with increased NET formation in response to neutrophil stimulation in MPN patients and in *Jak2*^{V617F} mouse models. Although a previous study indicated that neutrophils from patients with MPN have impaired in vitro NET formation when stimulated with cytokines (*33*), our study demonstrates increased NET formation in vitro in both *Jak2*^{V617F} human and mouse neutrophils in response to ionomycin. Such apparently discrepant results may be the result of the different stimuli used, including the selective use of specific inflammatory cytokines in the previous study. In addition, this previous report indicated that circulating nucleosomes, one source of which is NETs, were increased in blood samples from individuals with MPNs, although the authors propose that the nucleosomes are not NET-derived in this setting. Moreover, we performed in vivo experiments and found that increased NET formation is associated with increased thrombosis in *Jak2*^{V617F} mice, and both NET formation and thrombosis were dependent on PAD4, an enzyme essential for citrullination of histones. Treatment with ruxolitinib, a JAK1/2 inhibitor, abrogated NET formation in vitro and decreased thrombosis in *Jak2*^{V617F} mice in vivo.

The thrombogenic effect of the *Jak2*^{V617F} phenotype was apparent in NET-dependent venous murine thrombosis models, but not in a full ligation stasis model. These models rely principally on different components of the coagulation system and highlight the important point that there is no single murine venous thrombosis model that completely and faithfully simulates all aspects of human thrombosis. Furthermore, although we hypothesize that activation of the JAK-STAT
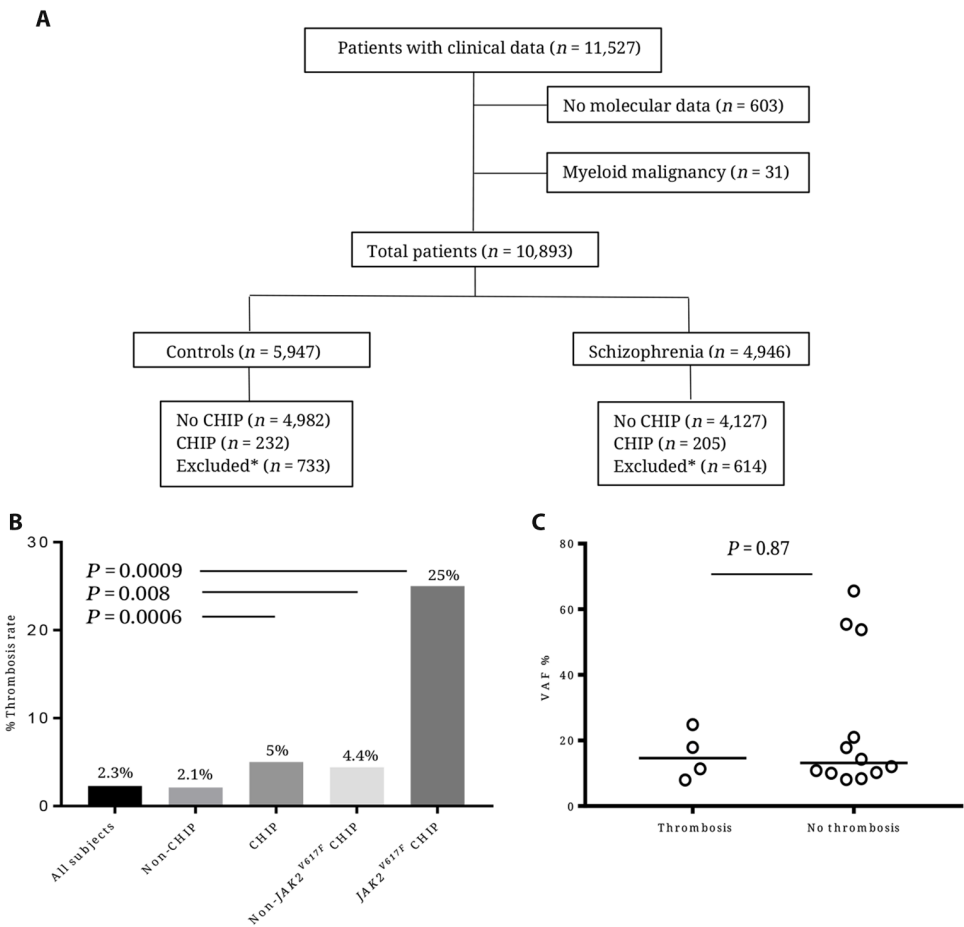
Wolach *et al.*, *Sci. Transl. Med.* **10**, eaan8292 (2018)   11 April 2018

5 of 10

Fig. 4. $JAK2^{V617F}$-positive clonal hematopoiesis is associated with increased thrombosis rates. (**A**) CONSORT (Consolidated Standards of Reporting Trials) diagram of individuals in the population study. (**B**) Rates of venous thrombosis in patients with or without CHIP and/or $JAK2^{V617F}$ mutation. (**C**) VAF of individuals with $JAK2^{V617F}$ CHIP separated according to the incidence of venous thrombosis.

Table 1. Comparison of incidence of venous thrombosis between groups according to the presence of CHIP and $JAK2^{V617F}$ mutation.

Analysis group*†	Control P value‡	Schizophrenia P value‡	All P value‡
Non-CHIP versus CHIP	0.0006 (0.003)	0.11	0.0004 (0.002)
Non-CHIP versus non-$JAK2^{V617F}$ CHIP	0.008 (0.04)	0.57	0.025 (0.125)
Non-CHIP versus $JAK2^{V617F}$ CHIP	0.0009 (0.0045)	0.12	0.0003 (0.0015)

*Individuals with fewer than three mutations of unknown significance were excluded from further analysis. Individuals with three or more mutations of unknown significance are classified as having clonal hematopoiesis with unknown driver (see also table S5). †Rates of thrombosis compared between groups by Fisher's exact test. ‡Nominal P values are given first. Adjusted P values after Bonferroni correction are given in parentheses.

pathway may serve as an endogenous regulator of NET formation, we have not defined where the JAK-STAT pathway fits in the currently accepted models of NET activation. Finally, although we have shown a clear association between $JAK2^{V617F}$ CHIP and venous thrombosis, our study is insufficiently powered to determine the importance of VAF in relation to the risk of thrombosis. This would be important for assessing which individuals may benefit from pharmacologic intervention, such as with ruxolitinib, designed to reduce the incidence or recurrence of thrombosis.

Ruxolitinib is currently U.S. Food and Drug Administration (FDA)–approved for the treatment of intermediate- and high-risk myelofibrosis and hydroxyurea-refractory PV (*34, 35*). In the RESPONSE trial, a large phase 3 study that resulted in the FDA approval of ruxolitinib for patients with PV not responding or intolerant to hydroxyurea, it is notable that there was a lower rate of thromboembolic events in the ruxolitinib-treated group (1.2 per 100 patient-years with ruxolitinib versus 2.8 for patients treated with other therapies) (*34*). In aggregate, our results suggest that JAK-STAT inhibition may have therapeutic utility in reducing NET formation and venous thrombosis in patients with MPNs including PV and also in individuals with $JAK2^{V617F}$-mutant CHIP.

MATERIALS AND METHODS
Study design
The aim of this study was to assess whether neutrophils harboring a $JAK2^{V617F}$ mutation had an increased propensity to form NETs and whether this was linked to an increased incidence of venous thrombosis. In addition, we sought to assess whether NETosis and subsequent thrombosis could be abrogated using clinically available inhibitors of JAK-STAT signaling.

We performed ex vivo assessment of mouse and human neutrophils with either $JAK2^{WT}$ or $JAK2^{V617F}$ with and without ruxolitinib treatment. NET formation was quantified before and after neutrophil stimulation using DAPI to detect morphological changes and IF to detect $H3^{cit}$ expression in the cells. Two different in vivo models of thrombosis (partial ligation and full ligation of the mouse IVC) were used to assess rates of thrombosis (at 4 hours unless otherwise stated) in both $Jak2^{WT}$ and $Jak2^{V617F}$ backgrounds. The impact of treatment with either ruxolitinib or DNase on the rate of thrombosis and on the composition of thrombi was also assessed in the partial ligation (NET-dependent) model. A potential role for PAD4, a protein required for NETosis, was assessed in patient samples and in a $Jak2^{V617F}$/Pad4 null mouse model. Finally, we assessed the incidence of venous thrombosis in individuals without a known myeloid disorder with $JAK2^{V617F}$ clonal hematopoiesis.

In all studies, mice were randomly assigned to control or treatment groups. The assessment and quantification of IHC and IF staining were performed blinded to the genetic and treatment conditions.

Experiments were done in triplicate. Sample sizes were based on previous studies comparing thrombosis rates between genetic/treatment groups using the same thrombosis models (36). No outliers were excluded. Primary data are reported in table S6.

Human blood samples
Blood was drawn from patients with MPNs and MDSs who were seen at the Dana-Farber Cancer Institute and from age-matched normal controls. Whole blood was collected into EDTA-coated tubes. Patients and controls were excluded if they had conditions that are known or suspected to affect NET formation such as active infection, active cancer (37), history of an autoimmune disease (38), treatment with immunosuppressive or anti-inflammatory drugs, or history of diabetes (29). In addition, patients with recent history of infection, trauma, or surgery (3 months before blood draw) were excluded. Therapy with acetylsalicylic acid (aspirin), hydroxyurea, or anagrelide was allowed. All patients and controls gave their written consent, and all blood samples were acquired according to protocols approved by the Dana-Farber Cancer Institute and Brigham and Women's Hospital Institutional Review Board.

Human neutrophil isolation and NET formation assay
Neutrophil isolation and NET formation were carried out as previously described (39). Briefly, blood was drawn from patients and normal controls into EDTA-coated tubes and was processed within 3 hours. RBCs were first sedimented with Hetastarch [6% hydroxyethyl starch (HES)] in 0.9% NaCl solution at 1:4 (v/v) dilution at 37°C and then was resuspended in RPMI 1640 (Corning) supplemented with 2% fetal bovine serum (FBS; Omega Scientific). The supernatant was harvested, and neutrophils were isolated using Percoll Plus (GE Healthcare) as previously described (39). Purity of cells was >95% as determined by Wright-Giemsa staining (fig. S1B). For the screening NET assay, NET-bound neutrophil elastase was quantified using an available commercial kit according to the manufacturer's instructions (Cayman Chemical). For the validation IF assay, neutrophils were resuspended in 2% heat-inactivated FBS and plated at 15,000 cells per well in 96-well optical-bottom plates in triplicate (Nunc MicroWell 96-Well Optical-Bottom Plates, Thermo Fisher Scientific). Cells were then stimulated with ionomycin at 4 μM (Sigma-Aldrich) or PMA at 10 and 100 nM (Sigma-Aldrich) for 2.5 hours. Cells were then instantly fixed in 2% paraformaldehyde (PFA) and stained as described below.

Mouse neutrophil isolation and NET formation assay
We used a previously published *VavCre/Jak2*[V617F] murine model that results in constitutive heterozygous expression of the *Jak2*[V617F] activating mutation (18). Peripheral blood was collected from 10- to 12-week-old mice via the retro-orbital venous plexus and was processed within 2 hours. RBCs were first sedimented with Hetastarch (6% HES) in 0.9% NaCl solution at 1:4 (v/v) dilution at 37°C. Next, supernatant was collected and subjected to brief hypotonic lysis with sterile water. Neutrophils were isolated by negative selection with magnetic beads according to the manufacturer's instructions (Neutrophil Isolation Kit, mouse; Miltenyi Biotec) and resuspended in 2% heat-inactivated FBS. Neutrophils were plated at 10 to 15,000 cells per well in 96-well optical-bottom plates in triplicate (Nunc MicroWell 96-Well Optical-Bottom Plates, Thermo Fisher Scientific). Cells were then stimulated with 4 μM ionomycin (Sigma-Aldrich) or 10 and 100 nM PMA (Sigma-Aldrich) for 2.5 hours. Cells were then instantly fixed in 2% PFA and stained as described below.

Immunostaining, fluorescence microscopy, and NET quantification
Fixed cells were processed as detailed above. Immunostaining, fluorescence microscopy, and NET quantification procedures were similar for human and mouse specimens. Samples were washed with phosphate-buffered saline (PBS) and permeabilized (0.1% Triton X-100 and 0.1% sodium citrate) for 10 min at 4°C. Samples were blocked with 3% bovine serum albumin (BSA) for 90 min at 37°C, rinsed, and then incubated overnight at 4°C or for 1 hour at 37°C in antibody dilution buffer containing 0.3% BSA, 0.1% Tween 20, and either rabbit anti–histone H3 (citrulline 2, 8, and 17) (0.3 μg/ml, ab5103; Abcam) or rat anti-Ly6G (0.5 μg/ml, clone 1A8; BioLegend). After three washes, samples were incubated for 2 hours at room temperature in antibody dilution buffer containing Alexa Fluor–conjugated secondary antibodies in 0.3% BSA in PBS: goat anti-rat immunoglobulin G (IgG) (Alexa 555, 2 μg/ml) or donkey anti-rabbit IgG (Alexa 488, 1.5 μg/ml). DNA was counterstained with DAPI (1 μg/ml), and slides were coverslipped with Fluoromount gel (Electron Microscopy Sciences).

Images were acquired on an Axiovert 200M wide-field fluorescence microscope (Zeiss) coupled to an AxioCam MR3 monochromatic charge-coupled device camera (Zeiss) using a Zeiss Plan-Neofluar 20×/0.4 Corr Ph2 objective lens with the Zeiss AxioVision software (version 4.6.3.0). Neutrophils positive for H3[cit] were determined by thresholding analysis using ImageJ software (National Institutes of Health).

Morphologic quantification of NETs was performed on the basis of morphological criteria that included nuclear delobulation and swelling and/or observed extension of web-like DNA strands. Percentages of H3[cit] cells and NETs were determined from five or six nonoverlapping fields per well, and the average was taken from duplicates or triplicates for each condition in every experiment. Exposure time for H3[cit] and DNA was identical for all treatments within the same experiment.

Results are expressed as percent NETs of DAPI-positive neutrophils. NET quantification was assessed independently by two investigators blinded to the conditions (O.W. and R.S.S.). Results obtained by the first investigator were independently verified by a second investigator blinded to the results.

Organ harvest and staining
Mice were sacrificed and injected immediately post-mortem via the trachea with a 50:50 mixture of 10% neutral-buffered formalin and optimal cutting temperature (OCT) compound (Sakura Finetek). Lungs were then removed and preserved in 10% neutral-buffered formalin solution for at least 24 hours before being processed for staining. Organs were embedded in paraffin, sectioned, rehydrated, and stained at the pathology research core facility at Harvard Medical School in Boston, MA.

Lung tissue to be used for IF was prepared for harvest in a similar manner as above but was embedded in OCT and snap-frozen immediately after harvest. Cryosections (10 μm) were then produced for staining. The Martius Scarlet Blue (MSB; trichrome) stains were performed on frozen sections fixed in Bouin's solution at 56°C for 1 hour and stained with an MSB kit per the manufacturer's instructions (Atom Scientific).

IF of thrombus and lung cryosections
Sections were allowed to come to room temperature, before rinsing in PBS with 0.1% Tween 20 (PBST). Sections were blocked for 1 hour at room temperature with 10% FBS in PBST in a humidified chamber. Sections were incubated in the same chamber overnight at 4°C

with the primary antibodies described above against Ly6G and H3[cit] or rat anti-CD41 [MWReg30 clone (recognizes integrin α2b), BioLegend catalog number 133901] in 10% FBS in PBST. Slides were rinsed in PBST before incubating with the secondary antibody under the same conditions as used for the primary antibody [goat anti-rat Ig (IgG) (Alexa 555, 1.5 μg/ml) or donkey anti-rabbit IgG (Alexa 647, 1.5 μg/ml)]. After a further wash in PBST, sections were stained with DAPI and mounted as described above. Sections were visualized using Axio Imager D1 (Carl Zeiss Microscopy), and images were taken using Axiocam MRc Camera (Carl Zeiss Microscopy). Zen software 2.3 (version 13) was used to analyze images. For the final images used in the figures, Alexa 647 was represented using green.

Venous stenosis model
After bone marrow harvest, c-Kit–positive marrow cells were obtained from *VavCre/Jak2*[V617F] KI mice using CD117 MicroBeads according to the manufacturer's instructions (Miltenyi Biotec). After being resuspended in Hanks' balanced salt solution (HBSS) (Life Technologies), cells were injected into lethally irradiated wild-type (WT) recipients [8-week-old female CD45.1-positive B6.SJL (Jackson Laboratory) recipients; 350,000 per animal], resulting in constitutive heterozygous expression of the mutation in hematopoietic cells only. Successful engraftment was checked using donor chimerism, as assessed by relative abundance of hematopoietic cells detected with either CD45.1-phycoerythrin (PE) clone A20 or CD45.2–fluorescein isothiocyanate (FITC) clone 104 (eBioscience), and a phenotype reminiscent of PV was documented (fig. S2).

Mice were anesthetized with 3.5% isoflurane, and isoflurane was maintained at 2% in 100% oxygen. A midline laparotomy was performed, and the IVC was exposed. Any side branches between the renal and iliac veins were ligated with 7/0 polypropylene suture. A 30-gauge spacer was placed parallel to the IVC, and 7/0 polypropylene suture was used to partially ligate the IVC to ~10% of its original diameter. The spacer was removed, and the mouse was sutured and allowed to recover. In the full ligation model, side branches were ligated as before. In addition, posterior branches were cauterized before the IVC was fully ligated with 7/0 polypropylene suture. At the designated post-ligation time points (2 and 4 hours), mice were anesthetized with isoflurane, and blood was collected via the retro-orbital sinus plexus. After the mice were sacrificed, the IVC was exposed to allow for collection of the thrombi formed within the IVC. The thrombi were embedded in OCT and snap-frozen for cryosectioning. All mice were given buprenorphine (0.03 μg/ml, v/v) (0.1 mg/kg) subcutaneously as an analgesic immediately before surgery.

Pad4 null *Jak2*[V617F] model
The previously published *Jak2*[V617F] murine stem cell virus (MSCV)–internal ribosomal entry site (IRES)–green fluorescent protein (GFP) vector (*27*) was used to generate ecotropic retrovirus using packaging plasmid (Ecopak), TransIT-LT1 Transfection Reagent (Mirus Bio LLC), and the human embryonic kidney cell line 293T using standard methods. Briefly, 293T cells were cultured in Dulbecco's modified Eagle's medium (DMEM; Corning) supplemented with 10% FBS and 1% penicillin/streptomycin/glutamine (PSG; Life Technologies). A total of 1.5 million cells were plated on a 10-cm plate. When cells were at 60 to 80% confluency, a transfection cocktail of 1 ml of reduced serum medium (Opti-MEM, Life Technologies), 45 μl of TransIT-LT1 Transfection Reagent, 10 μg of MSCV-IRES-GFP vector, and 10 μg of Ecopak vector was added to the plate. Medium containing the transfection mixture was removed after 12 hours. Fresh DMEM with

10% FBS and 1% PSG was added. After 36 hours, the medium (containing retrovirus) was harvested and filtered (22 μm). Bone marrow from *Pad4* null mice and *Pad4* WT controls was harvested, and c-Kit cells were isolated using CD117 MicroBeads as described above. Cells were cultured in serum-free expansion medium (StemSpan SFEM, Stem Cell Technologies) with recombinant murine thrombopoietin (50 ng/ml, PeproTech), recombinant murine stem cell factor (50 ng/ml, PeproTech), and 1% PSG for 48 hours. Cells were then transduced with fresh retrovirus using RetroNectin (Takara Bio Inc.) according to the manufacturer's instructions. After 24 hours, cells were resuspended in HBSS before transplantation of 350,000 cells by retro-orbital injection into lethally irradiated 8-week-old female CD45.1-positive B6.SJL (Jackson Laboratory) recipients. At 8 weeks after transplant, expression of viral construct was confirmed by assessing GFP using BD FACSCanto II (BD Biosciences), and HCT was assessed in animals by retro-orbital bleeding. The lungs from mice in the context of either *Pad4*^{−/−} or *Pad4*^{+/+} were harvested and processed for IHC and IF as described above.

Western blot analysis
After collection of human neutrophils, the samples were snap-frozen and homogenized in radioimmunoprecipitation assay buffer supplemented with protease inhibitor cocktail (Sigma-Aldrich) on ice. After centrifugation at 20,000g for 20 min at 4°C, equal amounts of protein per sample were resolved on Criterion 4 to 15% tris-HCl gels (Bio-Rad) and electroblotted on Immobilon-P polyvinylidene difluoride membranes (Merck Millipore), which were then incubated with primary antibodies (rabbit polyclonal anti-H3Cit, 1:1000, Abcam, catalog no. ab5103; mouse monoclonal anti-human PAD4, 1:1000, Abcam, catalog no. ab128086) at 4°C overnight and subsequently with appropriate horseradish peroxidase (HRP)–conjugated secondary antibodies [1:15,000, donkey anti-rabbit IgG (H+L)-HRP conjugate (GE Healthcare)] for 1 hour at room temperature. The blots were developed with SuperSignal West Dura Extended Duration Substrate enhanced chemiluminescence substrate (Thermo Fisher Scientific). Equal loading was confirmed using an HRP-conjugated monoclonal antibody against human β-actin (mAbcam 8226).

Treatment with ruxolitinib
For ex vivo experiments, ruxolitinib (Selleckchem) was used at a concentration of 300 nM for 150 min. For in vivo experiments, mice were gavaged with ruxolitinib (90 mg/kg) or vehicle (5% dimethylacetamide, Sigma-Aldrich) twice daily for 3 days (six doses) as previously described (*40*). For the ex vivo NET inhibition assay, we used a PAD4 inhibitor (GSK484 at 10 μM) as a negative control (Cayman Chemical).

Treatment with DNase
DNase 1 (Pulmozyme, Genentech) was diluted in sterile saline and injected immediately after surgery (50 μg intraperitoneally and 10 μg intravenously via tail vein). Control mice were injected with the DNase vehicle buffer [sodium chloride (8.77 mg/ml) and calcium chloride (0.15 mg/ml)] diluted in sterile saline. Mice were assessed for thrombosis at 4 hours.

Analysis of mouse plasma
Plasma dsDNA was analyzed using the Quant-iT PicoGreen assay (Invitrogen) according to the manufacturer's instructions.

Platelet and neutrophil functions
Mouse blood was collected in tubes containing enoxaparin (0.2 μg/ml) (Sanofi-Aventis). Platelet-rich plasma (PRP) was collected after two

centrifugation steps at 300g for 7 min at room temperature. ADP-induced aggregation was monitored in PRP, whereas responses after stimulation with thrombin or collagen were analyzed in washed platelet suspensions. For this, PRP was pelleted at 700g in the presence of prostacyclin (PGI$_2$) (0.1 μg/ml) and apyrase (0.02 U/ml). Platelet pellets were washed twice in modified Tyrode-Hepes buffer [134 mM NaCl, 0.34 mM Na$_2$HPO$_4$, 2.9 mM KCl, 12 mM NaHCO$_3$, 5 mM Hepes, 1 mM MgCl$_2$, 5 mM glucose, and 0.35% BSA (pH 7.4)] containing PGI$_2$ and apyrase. Platelet suspensions (150 μl with 5×10^5 platelets/μl) in Tyrode-Hepes buffer containing 2 mM CaCl$_2$ were stimulated with the indicated agonists, and light transmission was recorded on a Chrono-log platelet aggregometer.

For the assessment of CD11b induction, whole blood from $Jak2^{WT}$ or $Jak2^{V617F}$ mice that had been treated for 72 hours with either ruxolitinib or vehicle was processed as above to isolate neutrophils. After 20 min of stimulation with 4 μM ionomycin, neutrophils were stained with anti-mouse Ly6G APC antibody clone 1A8 (BioLegend) and anti-mouse CD11b FITC clone M1/70 (Invitrogen) and analyzed by flow cytometry (BD FACSCanto II). CD11b expression was quantified as the mean fluorescence intensity (MFI) of FITC in LyG-positive single cells. ROS were quantified after 20 min of stimulation with 4 μM ionomycin before staining with DHR-123 (Invitrogen) and anti-mouse Ly6G APC antibody clone 1A8 (BioLegend) at 4°C on ice. ROS concentrations were determined as the MFI of FITC for Ly6G-positive single cells.

Case-control cohort

Schizophrenic patients and controls from a case-control cohort were assessed, including only patients with both molecular and clinical data. Clinical data were assessed using the ICD-10 (International Statistical Classification of Diseases and Related Health Problems, 10th Revision) codes for different categories of major venous thrombosis and for myeloid disease including MPN, MDS, and AML (acute myeloid leukemia). ICD-10 codes and the corresponding diagnoses are shown in table S4. Individuals were regarded as being in one of two clinical groups: ever or never having had a venous thrombosis. Because previous data from this cohort suggested an effect of smoking on increased vascular events, and there were higher rates of smoking in the cohort of patients with schizophrenia, the schizophrenic patients and control cases were also assessed separately. Whole-exome sequencing, and the identification of mutations and their VAF, has been described previously (31).

Statistics

Data are presented as means ± SEM unless otherwise noted and were analyzed using a two-tailed Mann-Whitney U test. For murine data, thrombus frequencies were analyzed using Fisher's exact test. For human population, differences in thrombosis incidence were assessed using Fisher's exact test with Bonferroni correction for testing of multiple hypotheses. Differences in age were assessed using Mann-Whitney U test. All analyses were performed using GraphPad Prism software (version 5.0). Results were considered significant at $P < 0.05$. Nominal P values were used unless otherwise specified.

SUPPLEMENTARY MATERIALS

www.sciencetranslationalmedicine.org/cgi/content/full/10/436/eaan8292/DC1
Fig. S1. Complementary studies of NET formation in neutrophils derived from MPN patients.
Fig. S2. Phenotype reminiscent of PV in mice with $Jak2^{V617F}$-driven MPN.
Fig. S3. Neutrophil, platelet, RBC, and fibrin thrombus content.
Fig. S4. The effect of DNase treatment on thrombosis rate in an IVC partial ligation thrombosis model.
Fig. S5. IVC full ligation thrombosis model in $Pad4^{+/+}$ and $Pad4^{-/-}$ mice.
Fig. S6. IVC full ligation thrombosis model in $Jak2^{WT}$ and $Jak2^{V617F}$ with and without ruxolitinib treatment.
Fig. S7. Neutrophil activation and ROS production in neutrophils from $Jak2^{WT}$ and $Jak2^{V617F}$ mice.
Fig. S8. Platelet function in $Jak2^{WT}$ and $Jak2^{V617F}$ mice.
Fig. S9. NET formation in neutrophils derived from mice engrafted with $Jak2^{V617F}$-expressing $Pad4^{+/+}$ or $Pad4^{-/-}$ cells.
Fig. S10. Blood cell counts from the $Pad4/Jak2^{V617F}$ retroviral bone marrow transplant model.
Fig. S11. Differences in age between persons with and without CHIP.
Table S1. Patient characteristics (not treated with JAK inhibitors).
Table S2. Patient characteristics (JAK inhibitor–treated).
Table S3. Comparing NET formation between groups.
Table S4. ICD-10 codes used to identify thrombosis in the case-control cohort.
Table S5. Summary of thrombosis rates in the case-control study broken down by cohort (schizophrenia versus healthy controls) and type of clonal hematopoiesis.
Table S6. Primary data file (provided in Excel format).

REFERENCES AND NOTES

1. T. Klampfl, H. Gisslinger, A. S. Harutyunyan, H. Nivarthi, E. Rumi, J. D. Milosevic, N. C. C. Them, T. Berg, B. Gisslinger, D. Pietra, D. Chen, G. I. Vladimer, K. Bagienski, C. Milanesi, I. C. Casetti, E. Sant'Antonio, V. Ferretti, C. Elena, F. Schischlik, C. Cleary, M. Six, M. Schalling, A. Schönegger, C. Bock, L. Malcovati, C. Pascutto, G. Superti-Furga, M. Cazzola, R. Kralovics, Somatic mutations of calreticulin in myeloproliferative neoplasms. *N. Engl. J. Med.* **369**, 2379–2390 (2013).
2. T. Barbui, G. Finazzi, A. Falanga, Myeloproliferative neoplasms and thrombosis. *Blood* **122**, 2176–2184 (2013).
3. A. M. Vannucchi, P. Guglielmelli, JAK2 mutation-related disease and thrombosis. *Semin. Thromb. Hemost.* **39**, 496–506 (2013).
4. T. Barbui, A. Masciulli, M. R. Marfisi, G. Tognoni, G. Finazzi, A. Rambaldi, A. Vannucchi, White blood cell counts and thrombosis in polycythemia vera: A subanalysis of the CYTO-PV study. *Blood* **126**, 560–561 (2015).
5. R. Landolfi, L. Di Gennaro, T. Barbui, V. De Stefano, G. Finazzi, R. Marfisi, G. Tognoni, R. Marchioli; European Collaboration on Low-Dose Aspirin in Polycythemia Vera (ECLAP), Leukocytosis as a major thrombotic risk factor in patients with polycythemia vera. *Blood* **109**, 2446–2452 (2007).
6. P. J. Campbell, C. MacLean, P. A. Beer, G. Buck, K. Wheatley, J.-J. Kiladjian, C. Forsyth, C. N. Harrison, A. R. Green, Correlation of blood counts with vascular complications in essential thrombocythemia: Analysis of the prospective PT1 cohort. *Blood* **120**, 1409–1411 (2012).
7. A. Carobbio, E. Antonioli, P. Guglielmelli, A. M. Vannucchi, F. Delaini, V. Guerini, G. Finazzi, A. Rambaldi, T. Barbui, Leukocytosis and risk stratification assessment in essential thrombocythemia. *J. Clin. Oncol.* **26**, 2732–2736 (2008).
8. T. Barbui, A. Carobbio, F. Cervantes, A. M. Vannucchi, P. Guglielmelli, E. Antonioli, A. Alvarez-Larrán, A. Rambaldi, G. Finazzi, G. Barosi, Thrombosis in primary myelofibrosis: Incidence and risk factors. *Blood* **115**, 778–782 (2010).
9. V. Buxhofer-Ausch, H. Gisslinger, J. Thiele, B. Gisslinger, H.-M. Kvasnicka, L. Müllauer, S. Frantal, A. Carobbio, F. Passamonti, E. Rumi, M. Ruggeri, F. Rodeghiero, M. L. Randi, I. Bertozzi, A. M. Vannucchi, E. Antonioli, G. Finazzi, N. Gangat, A. Tefferi, T. Barbui, Leukocytosis as an important risk factor for arterial thrombosis in WHO-defined early/prefibrotic myelofibrosis: An international study of 264 patients. *Am. J. Hematol.* **87**, 669–672 (2012).
10. M. Hurtado-Nedelec, M. J. Csillag-Grange, T. Boussetta, S. A. Belambri, M. Fay, B. Cassinat, M.-A. Gougerot-Pocidalo, P. M.-C. Dang, J. El-Benna, Increased reactive oxygen species production and p47phox phosphorylation in neutrophils from myeloproliferative disorders patients with JAK2 (V617F) mutation. *Haematologica* **98**, 1517–1524 (2013).
11. A. Falanga, M. Marchetti, Thrombosis in myeloproliferative neoplasms. *Semin. Thromb. Hemost.* **40**, 348–358 (2014).
12. M. Kushnir, H. W. Cohen, H. H. Billett, Persistent neutrophilia is a marker for an increased risk of venous thrombosis. *J. Thromb. Thrombolysis* **42**, 545–551 (2016).
13. B. D. Vadher, S. J. Machin, K. G. Patterson, C. Sukhu, H. Walker, Life-threatening thrombotic and haemorrhagic problems associated with silent myeloproliferative disorders. *Br. J. Haematol.* **85**, 213–216 (1993).
14. V. Brinkmann, U. Reichard, C. Goosmann, B. Fauler, Y. Uhlemann, D. S. Weiss, Y. Weinrauch, A. Zychlinsky, Neutrophil extracellular traps kill bacteria. *Science* **303**, 1532–1535 (2004).
15. K. Martinod, D. D. Wagner, Thrombosis: Tangled up in NETs. *Blood* **123**, 2768–2776 (2014).
16. A. L. Barnado, L. J. Crofford, J. C. Oates, At the Bedside: Neutrophil extracellular traps (NETs) as targets for biomarkers and therapies in autoimmune diseases. *J. Leukoc. Biol.* **99**, 265–278 (2016).

Wolach *et al.*, *Sci. Transl. Med.* **10**, eaan8292 (2018)   11 April 2018

9 of 10

17. Y. Wang, M. Li, S. Stadler, S. Correll, P. Li, D. Wang, R. Hayama, L. Leonelli, H. Han, S. A. Grigoryev, C. D. Allis, S. A. Coonrod, Histone hypercitrullination mediates chromatin decondensation and neutrophil extracellular trap formation. *J. Cell Biol.* **184**, 205–213 (2009).

18. A. Mullally, S. W. Lane, B. Ball, C. Megerdichian, R. Okabe, F. Al-Shahrour, M. Paktinat, J. E. Haydu, E. Housman, A. M. Lord, G. Wernig, M. G. Kharas, T. Mercher, J. L. Kutok, D. G. Gilliland, B. L. Ebert, Physiological Jak2V617F expression causes a lethal myeloproliferative neoplasm with differential effects on hematopoietic stem and progenitor cells. *Cancer Cell* **17**, 584–596 (2010).

19. K. Martinod, M. Demers, T. A. Fuchs, S. L. Wong, A. Brill, M. Gallant, J. Hu, Y. Wang, D. D. Wagner, Neutrophil histone modification by peptidylarginine deiminase 4 is critical for deep vein thrombosis in mice. *Proc. Natl. Acad. Sci. U.S.A.* **110**, 8674–8679 (2013).

20. A. Brill, T. A. Fuchs, A. S. Savchenko, G. M. Thomas, K. Martinod, S. F. De Meyer, A. A. Bhandari, D. D. Wagner, Neutrophil extracellular traps promote deep vein thrombosis in mice. *J. Thromb. Haemost.* **10**, 136–144 (2012).

21. T. A. Fuchs, A. Brill, D. Duerschmied, D. Schatzberg, M. Monestier, D. D. Myers Jr., S. K. Wroblewski, T. W. Wakefield, J. H. Hartwig, D. D. Wagner, Extracellular DNA traps promote thrombosis. *Proc. Natl. Acad. Sci. U.S.A.* **107**, 15880–15885 (2010).

22. H. Meng, S. Yalavarthi, Y. Kanthi, L. F. Mazza, M. A. Elfline, C. E. Luke, D. J. Pinsky, P. K. Henke, J. S. Knight, In vivo role of neutrophil extracellular traps in antiphospholipid antibody–mediated venous thrombosis. *Arthritis Rheumatol.* **69**, 655–667 (2017).

23. O. M. El-Sayed, N. A. Dwyer, C. E. Luke, M. Elfline, A. Laser, C. Hogaboam, S. L. Kunkel, P. K. Henke, Intact Toll-like receptor 9 signaling in neutrophils modulates normal thrombogenesis in mice. *J. Vasc. Surg.* **64**, 1450–1458.e1 (2016).

24. L. Lamrani, C. Lacout, V. Ollivier, C. V. Denis, E. Gardiner, B. Ho Tin Noe, W. Vainchenker, J.-L. Villeval, M. Jandrot-Perrus, Hemostatic disorders in a JAK2V617F-driven mouse model of myeloproliferative neoplasm. *Blood* **124**, 1136–1145 (2014).

25. H. D. Lewis, J. Liddle, J. E. Coote, S. J. Atkinson, M. D. Barker, B. D. Bax, K. L. Bicker, R. P. Bingham, M. Campbell, Y. H. Chen, C.-w. Chung, P. D. Craggs, R. P. Davis, D. Eberhard, G. Joberty, K. E. Lind, K. Locke, C. Maller, K. Martinod, C. Patten, O. Polyakova, C. E. Rise, M. Rüdiger, R. J. Sheppard, D. J. Slade, P. Thomas, J. Thorpe, G. Yao, G. Drewes, D. D. Wagner, P. R. Thompson, R. K. Prinjha, D. M. Wilson, Inhibition of PAD4 activity is sufficient to disrupt mouse and human NET formation. *Nat. Chem. Biol.* **11**, 189–191 (2015).

26. P. Li, M. Li, M. R. Lindberg, M. J. Kennett, N. Xiong, Y. Wang, PAD4 is essential for antibacterial innate immunity mediated by neutrophil extracellular traps. *J. Exp. Med.* **207**, 1853–1862 (2010).

27. G. Wernig, T. Mercher, R. Okabe, R. L. Levine, B. H. Lee, D. G. Gilliland, Expression of Jak2V617F causes a polycythemia vera-like disease with associated myelofibrosis in a murine bone marrow transplant model. *Blood* **107**, 4274–4281 (2006).

28. M. Leshner, S. Wang, C. Lewis, H. Zheng, X. A. Chen, L. Santy, Y. Wang, PAD4 mediated histone hypercitrullination induces heterochromatin decondensation and chromatin unfolding to form neutrophil extracellular trap-like structures. *Front. Immunol.* **3**, 307 (2012).

29. S. L. Wong, M. Demers, K. Martinod, M. Gallant, Y. Wang, A. B. Goldfine, C. R. Kahn, D. D. Wagner, Diabetes primes neutrophils to undergo NETosis, which impairs wound healing. *Nat. Med.* **21**, 815–819 (2015).

30. R. Rampal, F. Al-Shahrour, O. Abdel-Wahab, J. P. Patel, J.-P. Brunel, C. H. Mermel, A. J. Bass, J. Pretz, J. Ahn, T. Hricik, O. Kilpivaara, M. Wadleigh, L. Busque, D. G. Gilliland, T. R. Golub, B. L. Ebert, R. L. Levine, Integrated genomic analysis illustrates the central role of JAK-STAT pathway activation in myeloproliferative neoplasm pathogenesis. *Blood* **123**, e123–e133 (2014).

31. G. Genovese, A. K. Kähler, R. E. Handsaker, J. Lindberg, S. A. Rose, S. F. Bakhoum, K. Chambert, E. Mick, B. M. Neale, M. Fromer, S. M. Purcell, O. Svantesson, M. Landén, M. Höglund, S. Lehmann, S. B. Gabriel, J. L. Moran, E. S. Lander, P. F. Sullivan, P. Sklar, H. Grönberg, C. M. Hultman, S. A. McCarroll, Clonal hematopoiesis and blood-cancer risk inferred from blood DNA sequence. *N. Engl. J. Med.* **371**, 2477–2487 (2014).

32. S. Jaiswal, P. Fontanillas, J. Flannick, A. Manning, P. V. Grauman, B. G. Mar, R. C. Lindsley, C. H. Mermel, N. Burtt, A. Chavez, J. M. Higgins, V. Moltchanov, F. C. Kuo, M. J. Kluk, B. Henderson, L. Kinnunen, H. A. Koistinen, C. Ladenvall, G. Getz, A. Correa, B. F. Banahan, S. Gabriel, S. Kathiresan, H. M. Stringham, M. I. McCarthy, M. Boehnke, J. Tuomilehto, C. Haiman, L. Groop, G. Atzmon, J. G. Wilson, D. Neuberg, D. Altshuler, B. L. Ebert, Age-related clonal hematopoiesis associated with adverse outcomes. *N. Engl. J. Med.* **371**, 2488–2498 (2014).

33. C. P. Marin Oyarzún, A. Carestia, P. R. Lev, A. C. Glembotsky, M. A. Castro Ríos, B. Moiraghi, F. C. Molinas, R. F. Marta, M. Schattner, P. G. Heller, Neutrophil extracellular trap formation and circulating nucleosomes in patients with chronic myeloproliferative neoplasms. *Sci. Rep.* **6**, 38738 (2016).

34. A. M. Vannucchi, J. J. Kiladjian, M. Griesshammer, T. Masszi, S. Durrant, F. Passamonti, C. N. Harrison, F. Pane, P. Zachee, R. Mesa, S. He, M. M. Jones, W. Garrett, J. Li, U. Pirron, D. Habr, S. Verstovsek, Ruxolitinib versus standard therapy for the treatment of polycythemia vera. *N. Engl. J. Med.* **372**, 426–435 (2015).

35. S. Verstovsek, R. A. Mesa, J. Gotlib, R. S. Levy, V. Gupta, J. F. DiPersio, J. V. Catalano, M. Deininger, C. Miller, R. T. Silver, M. Talpaz, E. F. Winton, J. H. Harvey Jr., M. O. Arcasoy, E. Hexner, R. M. Lyons, R. Paquette, A. Raza, K. Vaddi, S. Erickson-Viitanen, I. L. Koumenis, W. Sun, V. Sandor, H. M. Kantarjian, A double-blind, placebo-controlled trial of ruxolitinib for myelofibrosis. *N. Engl. J. Med.* **366**, 799–807 (2012).

36. K. Martinod, T. Witsch, K. Farley, M. Gallant, E. Remold-O'Donnell, D. D. Wagner, Neutrophil elastase-deficient mice form neutrophil extracellular traps in an experimental model of deep vein thrombosis. *J. Thromb. Haemost.* **14**, 551–558 (2016).

37. M. Demers, D. S. Krause, D. Schatzberg, K. Martinod, J. R. Voorhees, T. A. Fuchs, D. T. Scadden, D. D. Wagner, Cancers predispose neutrophils to release extracellular DNA traps that contribute to cancer-associated thrombosis. *Proc. Natl. Acad. Sci. U.S.A.* **109**, 13076–13081 (2012).

38. D. Simon, H. U. Simon, S. Yousefi, Extracellular DNA traps in allergic, infectious, and autoimmune diseases. *Allergy* **68**, 409–416 (2013).

39. A. S. Gonzalez, B. W. Bardoel, C. J. Harbort, A. Zychlinsky, Induction and quantification of neutrophil extracellular traps. *Methods Mol. Biol.* **1124**, 307–318 (2014).

40. A. Quintás-Cardama, K. Vaddi, P. Liu, T. Manshouri, J. Li, P. A. Scherle, E. Caulder, X. Wen, Y. Li, P. Waeltz, M. Rupar, T. Burn, Y. Lo, J. Kelley, J. Covington, S. Shepard, J. D. Rodgers, P. Haley, H. Kantarjian, J. S. Fridman, S. Verstovsek, Preclinical characterization of the selective JAK1/2 inhibitor INCB018424: Therapeutic implications for the treatment of myeloproliferative neoplasms. *Blood* **115**, 3109–3117 (2010).

Science Translational Medicine

Increased neutrophil extracellular trap formation promotes thrombosis in myeloproliferative neoplasms

Ofir Wolach, Rob S. Sellar, Kimberly Martinod, Deya Cherpokova, Marie McConkey, Ryan J. Chappell, Alexander J. Silver, Dylan Adams, Cecilia A. Castellano, Rebekka K. Schneider, Robert F. Padera, Daniel J. DeAngelo, Martha Wadleigh, David P. Steensma, Ilene Galinsky, Richard M. Stone, Giulio Genovese, Steven A. McCarroll, Bozenna Iliadou, Christina Hultman, Donna Neuberg, Ann Mullally, Denisa D. Wagner and Benjamin L. Ebert

A NET increase in thrombosis

Excessive thrombosis is a major cause of complications in cancer, including myeloproliferative neoplasms. Neutrophil extracellular traps (NETs) are structures formed from DNA expelled by activated neutrophils in infection, autoimmune disease, or cancer, and these can be associated with thrombosis. Wolach *et al.* discovered that increased activity of a protein called JAK2 is associated with NET formation in myeloproliferative neoplasms and that inhibiting it with ruxolitinib, a drug that targets JAK2, decreases thrombosis in a mouse model. Moreover, in a data set from more than 10,000 people without myeloproliferative neoplasms, detection of a clonal population of blood cells with overactive JAK2 correlated with a risk of thrombotic events, suggesting a broader relevance for this finding beyond the setting of cancer.

ARTICLE TOOLS	http://stm.sciencemag.org/content/10/436/eaan8292
SUPPLEMENTARY MATERIALS	http://stm.sciencemag.org/content/suppl/2018/04/09/10.436.eaan8292.DC1
RELATED CONTENT	http://stm.sciencemag.org/content/scitransmed/10/429/eaam7729.full http://stm.sciencemag.org/content/scitransmed/3/76/76ra27.full http://stm.sciencemag.org/content/scitransmed/8/361/361ra138.full
REFERENCES	This article cites 40 articles, 18 of which you can access for free http://stm.sciencemag.org/content/10/436/eaan8292#BIBL
PERMISSIONS	http://www.sciencemag.org/help/reprints-and-permissions